Agricultural and Forest Meteorology 108 (2001) 55–65

AGRICULTURAL AND FOREST METEOROLOGY

www.elsevier.com/locate/agrformet

Estimation of surface sensible heat flux using dual angle observations of radiative surface temperature

A. Chehbouni [a,*], Y. Nouvellon [b], J.-P. Lhomme [c], C. Watts [d], G. Boulet [a], Y.H. Kerr [a], M.S. Moran [b], D.C. Goodrich [b]

[a] *CESBIO (CNES–CNRS–IRD–UPS), 18 Avenue Edouard Belin, 31401 Toulouse Cedex 4, France*
[b] *USDA–ARS–SWRC, Tuscon, AZ, USA*
[c] *CNRS–CEFE, Montpellier, France*
[d] *IMADES, Hermosillo, Sonora, Mexico*

Received 26 June 2000; received in revised form 2 January 2001; accepted 6 January 2001

Abstract

In this study, dual angle observations of radiative surface temperature have been used in conjunction with a two-layer model to derive sensible heat flux over a sparsely vegetated surface. Data collected during the semi-arid-land-surface-atmosphere program (SALSA) over a semi-arid grassland in Mexico were used to assess the performance of the approach. The results showed that this approach led to reasonable estimates of the observed fluxes. The mean average percentage difference (MAPD) between observed and simulated fluxes was about 23%, which is not statistically different from the expected 20% scatter, when different flux measuring devices are compared over the same site. However, the sensitivity analysis indicated that the approach was rather sensitive to uncertainties in both measured radiative temperatures and aerodynamic characteristics of the vegetation. Finally, the issue of using dual angle observations of surface temperature for characterizing the difference between aerodynamic and nadir viewing radiative temperature has been examined. The results showed that this difference is linearly correlated with the difference between nadir and oblique radiative temperatures. Based on this finding, we expressed sensible heat flux in terms of the (nadir) radiative-air temperature gradient and a corrective term involving the nadir–oblique temperature differences. This formulation has been successfully tested. The resulting MAPD was about 33%.

Keywords: Aerodynamic temperature; Directional radiative temperature; Two-layer model; Sensible heat flux; Gap fraction

1. Introduction

Substantial progress has been made towards taking full advantage of increasingly available remotely sensed data to improve the representation of surface processes in hydro-atmospheric models at different space-time scales (Arain et al., 1996; Bastiaansen et al., 1998; Avissar, 1998). However, the key issue is establishing, at different scales, relationships that link remote sensing observations to the variables needed to formulate surface fluxes (Njoku et al., 1996). In the case of sensible heat flux, it is the aerodynamic surface temperature, not the remotely sensed radiative surface temperature that determines the loss of sensible heat flux from the surface. Aerodynamic surface temperature is formally defined as the extrapolation of

* Corresponding author. Tel.: +33-5-6155-8523; fax: +33-5-6155-8500.
E-mail address: ghani@cesbio.cnes.fr (A. Chehbouni).

0168-1923/01/$ – see front matter
PII: S0168-1923(01)00221-0

the air temperature profile down to an effective height within the canopy at which the vegetation component of sensible heat flux arises (Kalma and Jupp, 1990).

As the aerodynamic surface temperature is usually unknown, one practical approach is to replace it with the radiative surface temperature in the sensible heat flux equation and to add a corrective term that takes into account the difference between these two temperatures. This corrective or adjustment term is derived through two functionally equivalent approaches that consist of either adding an "excess resistance" to the aerodynamic resistance (e.g. Kustas et al., 1989; Moran et al., 1994; Stewart et al., 1994), or directly modifying the temperature difference (e.g. Chehbouni et al., 1996, 1997). During the past two decades, a number of investigations have been directed towards documenting and predicting the behavior of this corrective term (e.g. Mathias et al., 1987; Hall et al., 1992; Kustas et al., 1990; Kubota and Sugita, 1994; Sugita and Kubota, 1994; Norman et al., 1995; Brutsaert and Sugita, 1996; Sugita and Brutsaert, 1996; Sun and Mahrt, 1995; Malhi, 1996; Lhomme et al., 1997, 2000; Verhoef et al., 1997; Troufleau et al., 1997; Cahill and Parlange, 1997; Crago, 1998; Massman, 1999; Blumel, 1999; Watts et al., 2000). Still, none of the reported approaches appear to be convincing; all of them are empirical and therefore difficult to apply a priori to different surface types (Chehbouni et al., 2000a). The key problem is that the departure of the aerodynamic temperature from the radiative temperature depends on a multitude of factors, such as vegetation type and condition, soil moisture status, and to a lesser extent, atmospheric variables (mainly wind speed and incoming radiation). Therefore, it is very difficult to find a robust relationship between aerodynamic temperature and a single-angle observation of radiative temperature that takes into account all these factors.

The above problem can be circumvented to some extent by using the so-called two-layer or two-source type models (Shuttleworth and Wallace, 1985; Shuttleworth and Gurney, 1990). In this type of model, the aerodynamic temperature is analytically expressed in terms of the component temperatures and a set of resistances. The use of these models for operational purposes has been somewhat limited by the fact that they require component surface temperatures (i.e. soil and vegetation) that could not be obtained from remote sensing measurements. Fortunately, progress in understanding the directional behavior of radiative surface temperature has been made. In this regard, several investigations have demonstrated the feasibility of obtaining soil and vegetation temperature using dual angle observations of directional radiative surface temperature (e.g. Francois et al., 1997; Chehbouni et al., 2000b). Thus, the availability of satellite-based dual-angle observations in thermal infrared bands with the Along Track Scanning Radiometer (ATSR) instrument, aboard the first European Remote Sensing Satellite (ERS-1; Prata, 1990) makes the derivation of component surface temperatures from space, and therefore, the use of dual-source models are possible (Kustas and Norman, 1997).

The objective of this study was to present an approach that combines dual angle observations of directional radiative temperature and the Shuttleworth and Gurney (1990) two-layer model for predicting instantaneous sensible heat flux values. The performance of the approach was assessed by comparing predicted versus observed turbulent fluxes made up over a semi-arid grassland site during the 1999 semi-arid-land-surface-atmosphere (SALSA) field campaign. The following sections provide a description of the thermal infrared radiative transfer model and the two-layer surface scheme, a presentation of the study site and data, an assessment of the performance and the robustness of this approach, and an investigation of the impact of uncertainties in measured directional temperature and in vegetation aerodynamic characteristics on the flux estimates. The study concludes with a discussion about the limitations of this approach with respect to operational applications and with new insights on the difference between directional radiative temperature and aerodynamic temperature.

2. Modeling background

2.1. Directional thermal radiative transfer model

The directional radiance $R_\lambda(\theta)$ observed by a radiometer in a direction θ, at a given wavelength λ, can be expressed, for a natural surface, as

$$R_\lambda(\theta) = \varepsilon(\lambda, \theta) B_\lambda(T_r) + [1 - \varepsilon(\lambda, \theta)]\mathrm{Ra}_\lambda \qquad (1)$$

where T_r is the directional radiative temperature of the surface, $B_\lambda(T_r)$ the Planck function, $\varepsilon(\lambda,\theta)$ the directional spectral emissivity, and Ra_λ the incoming long-wave radiation reaching the surface. In the following, the waveband reference will be omitted since a nominal 8–14 μm band pass was considered. The directional emissivity and the directional radiative temperature result from the contributions of the different surface elements seen by the sensor. These contributions are calculated using the directional gap frequency through the vegetation defined as

$$b(\theta) = \exp\left(-\lambda(\theta)\frac{G(\theta)}{\cos\theta}\mathrm{PAI}\right) \quad (2)$$

where PAI is the plant area index, the ratio $G(\theta)/\cos\theta$ represents the directional extinction coefficient for a canopy with a random leaf dispersion, and $\lambda(\theta)$ the directional leaf dispersion parameter that accounts for the canopy clumping (see, Nouvellon et al., 2000a; Chehbouni et al., 2000b for more details).

The thermal infrared radiative transfer model used in this study is both simple and widely used. It computes the directional radiance for a nominal band pass of the radiometer (8–14 μm here) in terms of soil and vegetation temperatures (T_s, T_v) and emissivities (ε_s, ε_v), incoming long-wave radiation (Ra), and the gap frequency function $b(\theta)$

$$R(\theta) = b(\theta)\varepsilon_s B(T_s) + [1 - b(\theta)]\,\varepsilon_v B(T_v) + [1 - \varepsilon_c(\theta)]\mathrm{Ra} \quad (3)$$

where $B(T)$ is the integrated Planck function and $\varepsilon_c(\theta)$ represents an average or effective canopy directional emissivity, which was computed here as the average of soil and vegetation emissivities weighted by the directional gap frequency as

$$\varepsilon_c(\theta) = b(\theta)\varepsilon_s + [1 - b(\theta)]\,\varepsilon_v \quad (4)$$

The values of soil and vegetation emissivity used in this study were 0.94 and 0.98, respectively. These values are similar to those reported following an experimental investigation performed by Humes et al. (1994) in the same basin. It is worthwhile to mention that the study performed by Chehbouni et al. (2001) showed that, despite its simplicity, the performance of this model with respect to inverting component surface temperatures was similar to more complex ones (Kimes, 1980, 1981; Prevot, 1985; Francois et al., 1997).

2.2. Dual-source energy balance model

The two-source model used in this study was developed by Shuttleworth and Wallace (1985) and modified by Shuttleworth and Gurney (1990). The basic idea behind this model is that the two sources of water vapor and heat are superimposed and hence heat and water enter or leave the bottom layer only via the top one. The total flux of sensible heat emanating from the whole surface is computed as the sum of the fluxes emanating from each layer (here soil and vegetation). According to the above representation, sensible heat flux can be written as

$$H = H_s + H_v = \frac{\rho C_p (T_0 - T_a)}{r_{aa}} \quad (5)$$

where ρ is the air density, C_p the specific heat of air at constant pressure, T_a the air temperature at the reference height (z_r), T_0 the aerodynamic temperature defined as the extrapolation of air temperature to the apparent source/sink of heat within the canopy, r_{aa} the aerodynamic resistance for heat transfer calculated between the level of apparent sink of momentum and the reference height. Soil (H_s) and vegetation (H_v) contributions to sensible heat flux can be expressed using the gradient-diffusion hypothesis as

$$H_s = \frac{\rho C_p (T_s - T_0)}{r_{as}} \quad (6)$$

$$H_v = \frac{\rho C_p (T_v - T_0)}{r_{ac}} \quad (7)$$

where T_s and T_v are soil and vegetation temperature, respectively, r_{as} the aerodynamic resistance between the soil and the source height and r_{ac} the bulk boundary-layer resistance of the vegetation. The aerodynamic resistance r_{aa} (assumed to be the same for heat and water vapor) is formulated using the classical expression which takes into account the stability correction functions for wind and temperature (Brutsaert, 1982)

$$r_{aa} = \frac{1}{ku_*}\left[\ln\left(\frac{z_r - d}{z_0}\right) - \boldsymbol{\Psi}_h(\boldsymbol{\zeta})\right] \quad (8)$$

with

$$u_* = \frac{ku_a}{\ln((z_r - d)/z_0) - \boldsymbol{\Psi}_m(\boldsymbol{\zeta})} \quad (9)$$

where u_* is the friction velocity, u_a the wind speed at the reference height, k the von Karman's constant, $\boldsymbol{\Psi}_h$ and $\boldsymbol{\Psi}_m$ are the stability correction functions for heat and momentum, respectively (Paulson, 1970). $\boldsymbol{\zeta} = (z_r - d)/L$, is a dimensionless parameter which reflects atmospheric stability as a function of the Obukhov length L. The zero plane displacement height d and the roughness length for momentum z_0 can be determined following Choudhury and Monteith (1988), who fitted simple functions to the curves obtained by Shaw and Pereira (1982) from second-order closure theory

$$d = 1.1h \ln(1 + X^{1/4}), \quad X = c_d\text{PAI} \quad (10)$$

$$z_0 = \begin{cases} z_{0s} + 0.3hX^{1/2}, & 0 < X < 0.2 \\ 0.3h(1 - d/h), & 0.2 < X < 1.5 \end{cases} \quad (11)$$

where c_d is the mean drag coefficient assumed to be uniform within the canopy (0.2), h the height of the canopy and z_{0s} the roughness length of the substrate. For bare soil, z_{0s} is commonly taken as 0.01 m (Shuttleworth and Wallace, 1985). The aerodynamic resistance between the substrate and the source height of the whole canopy $(d + z_0)$ is defined as the integral of the reciprocal of eddy diffusivity over the height range $[z_{0s}, d + z_0]$ (Choudhury and Monteith, 1988)

$$r_{as} = \frac{h \exp(\alpha_w)}{\alpha_w K(h)} \left\{ \exp\left[\frac{-\alpha_w z_{0s}}{h}\right] - \exp\left[\frac{-\alpha_w (d + z_0)}{h}\right] \right\} \quad (12)$$

where $K(h)$ is the value of eddy diffusivity at canopy height, $K(h) = ku_*(h - d)$. The bulk boundary-layer resistance of the canopy is calculated by integrating the leaf boundary-layer conductance over the canopy height (Choudhury and Monteith, 1988)

$$r_{ac} = \frac{\alpha_w [w/u(h)]^{1/2}}{4\alpha_0 \text{PAI}\,[1 - \exp(-\alpha_w/2)]} \quad (13)$$

where w is the leaf width, which was found to be 0.01 m here, $u(h)$ the wind speed at canopy height h, and α_w and α_0 the two constant coefficients equal to 2.5 (dimensionless) and 0.005 (m s$^{-1/2}$), respectively.

Finally, the following system of equations and can be solved numerically to obtain component temperatures and aerodynamic temperatures from which sensible heat flux can be computed.

$$R(\theta_1) = b(\theta_1)\varepsilon_s B(T_s) + [1 - b(\theta_1)]\varepsilon_v(T_v) + [1 - \varepsilon_c(\theta_1)]\text{Ra} \quad (14a)$$

$$R(\theta_2) = b(\theta_2)\varepsilon_s B(T_s) + [1 - b(\theta_2)\varepsilon_v B(T_v) + [1 - \varepsilon_c(\theta_2)]\text{Ra} \quad (14b)$$

$$\frac{T_0 - T_a}{r_{aa}} = \frac{T_s - T_0}{r_{as}} + \frac{T_v - T_0}{r_{ac}} \quad (14c)$$

3. Site and data description

The Upper San Pedro Basin was identified as the focus area for the SALSA program (Goodrich et al., 2000; Chehbouni et al., 2000b). The basin represents a transition area between the Sonoran and Chihuahuan deserts. It is an international basin spanning the Mexico–US border with significantly different cross-border legal and land use practices, as well as significant topographic and vegetation variation. Major vegetation types include desert grasslands, shrub-steppe, mesquite, oak Savannah, Pinyon-juniper, and Ponderosa pine.

For this particular study, the site was located near Zapata village in the Mexican portion of the basin (110°09′W; 31°01′N; elevation 1460 m) which was the center for SALSA activities in Mexico from 1997 to 1999. The natural vegetation is composed mainly of perennial sparse grasses, the dominant species being *Bouteloua* and *Eragrostis* spp. The soil is a sandy loam (67% sand and 12% clay).

A meteorological tower, equipped with micrometeorological instruments has been operated since 1997. This included wind speed and direction, air temperature and humidity which were measured at a height of 7.4 m. Soil heat flux was measured using six HFT3 plates (REBS, WA, USA), soil temperature and soil moisture were measured at different depths using six 108 temperature probes and six CS600 TDR (time domain reflectometer) probes, respectively (Campbell Scientific, USA). In 1999, the four components of net radiation were measured using a CNR1 (Kipp and Zonen) radiometer. The flux of water, energy and momentum were measured at a height of 6.7 m using an eddy correlation system. This included a 3D sonic anemometer, a fast response (fine wire) thermocouple and a fast response hygrometer (Campbell Scientific, USA). Directional surface temperature was measured using two 8–14 μm, infrared radio-thermometers (Everest Interscience, Model 4000), which were compared prior the experiment. One with a 60° field of view (FOV) was installed at 2.5 m height, aiming vertically at a representative spot. The second had a 15° FOV, and was installed at 3.33 m height, at an angle of 55° aimed at the same spot. It is certain that the use of the 60° (±30°) IRT does mean that significant off-nadir measurements are included which is undesirable. However, under the economic and technical conditions of the experiment, this seemed to be the only viable alternative for measuring a relatively large patch.

Green and senescent components of the biomass as well as the height of the vegetation were monitored once a week during the entire growing season. The PAI was determined from biomass values and plant specific area (PSA) measurements.

4. Results and discussion

Directional radiative temperature data collected at two angles ($\theta_1 = 0°$ and $\theta_2 = 55°$) from day of the year (DOY) 212–271 at 1200 local time (LT) were used in this study. During the study period, the PAI and the vegetation height varied from 0.4 to 1.1, and from 0.2 to 0.7 m, respectively. The soil moisture values ranged from a minimum 0.05 to a maximum of 0.18. This lead to values of evaporative fraction, defined as the ratio of latent heat flux to available energy, ranging from 0.2 to 0.8. In Fig. 1, the cross-plot of the difference between nadir and oblique radiative temperature and the PAI throughout the study period is presented. The departure of nadir from off-nadir radiative temperature varies non-linearly with the PAI. One possible explanation of the observed "U" shape can be explained by the fact that the contrast between soil and vegetation temperatures which is the main driver of the departure of nadir from off-nadir radiative temperature decreases with increasing surface soil moisture (see Chehbouni et al. (2001) for more details).

Dual angle observations of radiative surface temperature (0 and 55°C) have been used in conjunction with ancillary meteorological data and vegetation aerodynamic characteristics, to investigate the effectiveness of the approach outlined in Section 2. The performance of the approach was evaluated using different measures suggested by Norman et al. (1995). This included the root mean square differences (RMSDs), and the mean absolute difference (MAD) and the mean absolute percent difference (MAPD). The MAPD allows comparisons with the typical uncertainties

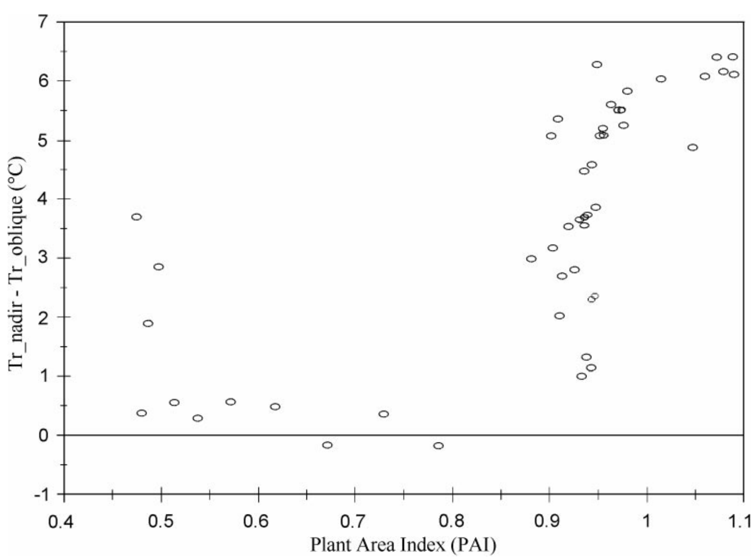

Fig. 1. Cross-plot of the difference between nadir and oblique radiative temperature and the PAI throughout the study period.

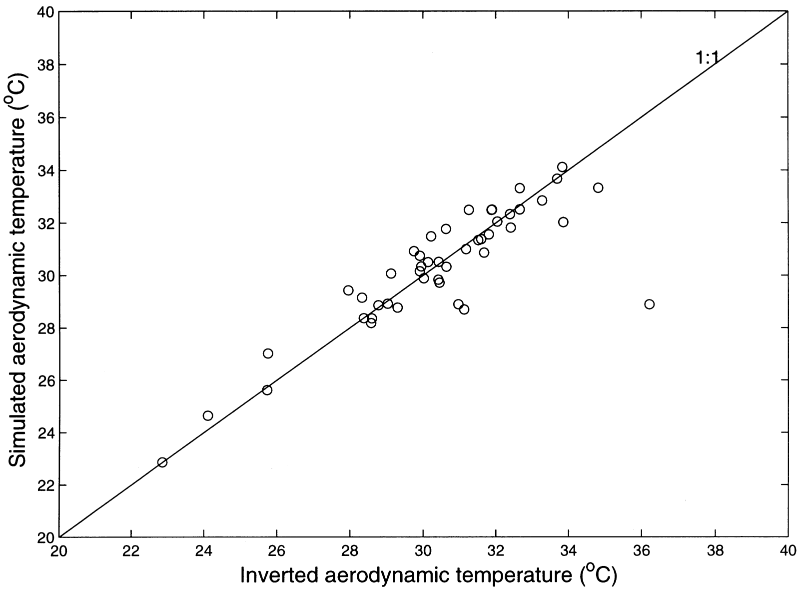

Fig. 2. Comparison between simulated and inverted aerodynamic temperature (°C).

found in the micro-meteorological techniques (Kustas and Norman, 1997).

Aerodynamic surface temperatures were inverted from Eq. (5) using measured sensible heat flux values and estimates of aerodynamic resistance. Apart from a few outliers that might be due to clouds or to instrumental problems, the model reproduced fairly accurately (MAPD of 2.5%) the inverted values of T_0 (Fig. 2). Similarly, the MAPD between measured and simulated sensible heat flux value (Fig. 3) was about

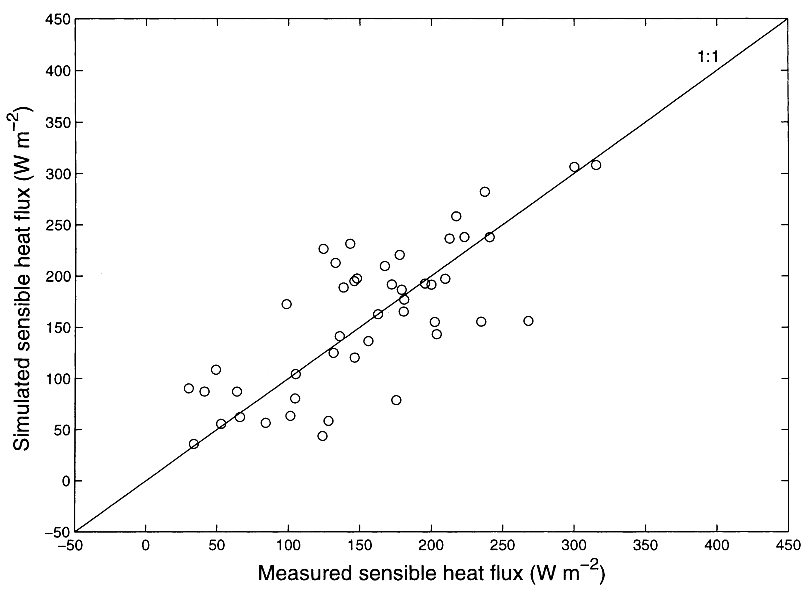

Fig. 3. Comparison between simulated and measured sensible heat flux values ($W\,m^{-2}$).

Table 1
Performance statistics of the approach

Variables	MAD ($W m^{-2}$ or K)	MAPD (%)	RMSD ($W m^{-2}$ or K)
Sensible heat flux	35	23	47
Aerodynamic temperature	0.75	2.46	1.35

%, which is similar to the variation encountered (20%) when different flux measurement systems are inter-compared (Kustas and Norman, 1997). The performance statistics in Table 1 represent an improvement with respect to those reported in a similar study performed by Kustas and Norman (1997), where measurements of dual angle observations of directional temperature were also used in conjunction with a different two-source model (more than 50%). Bearing in mind the mismatch between the footprint of the infrared radiometers and the area representative of the flux measurements, the performance of this approach was deemed acceptable. Consequently, the possibility of obtaining component temperatures from dual angle satellite observations in the thermal infrared bands makes the prospect of applying the current approach for routinely monitoring surface sensible heat flux potentially attractive.

However, this approach for estimating surface fluxes requires high accuracy of directional radiative temperature (to a better than 1 K). An error of 1 K in the measured directional temperatures translates, in our case, into an error of about 1.03 and 2.25 K for soil and vegetation temperature, respectively. This leads to a deviation of about 40% in sensible heat flux values. Additionally, the aerodynamic characteristics of the vegetation also need to be accurately known. As an example, a change from 2.5 to 2 of the constant α_w (Eq. (12)), which represents the exponential decay of eddy diffusivity, translates into a 20% variation of the flux. The required accuracy for both directional radiative temperature measurements and aerodynamic characteristics of the vegetation which is still difficult to be achieved from satellite observations, may represent a drawback for operational application.

To provide new insights of the relationship between aerodynamic and nadir viewing radiative surface temperature, differences between aerodynamic and radiative temperature observed at nadir were plotted against differences between soil and vegetation temperatures (Fig. 4). As expected, this figure indicates that there is a relationship between the two quantities. This feature can be explained by the fact that the departure of aerodynamic from nadir viewing radiative surface temperature is mainly controlled by soil moisture

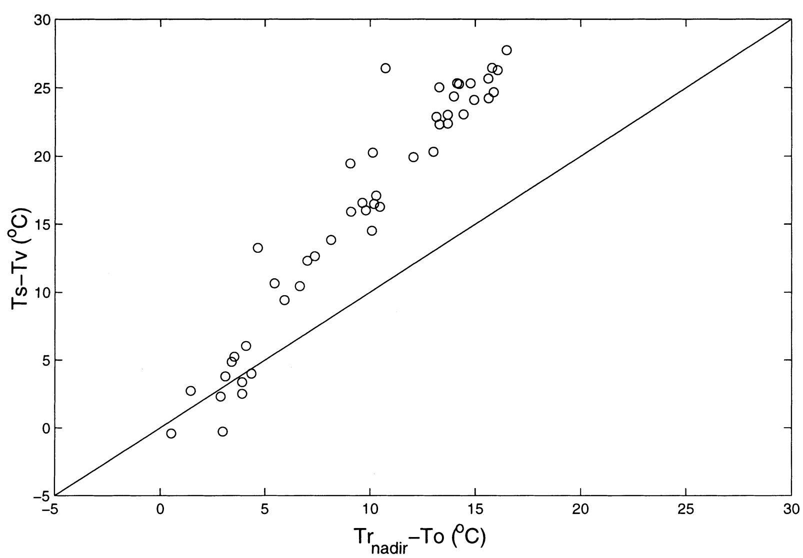

Fig. 4. Cross-plot of the difference between nadir viewing radiative and aerodynamic surface temperatures and the difference between soil and vegetation temperatures.

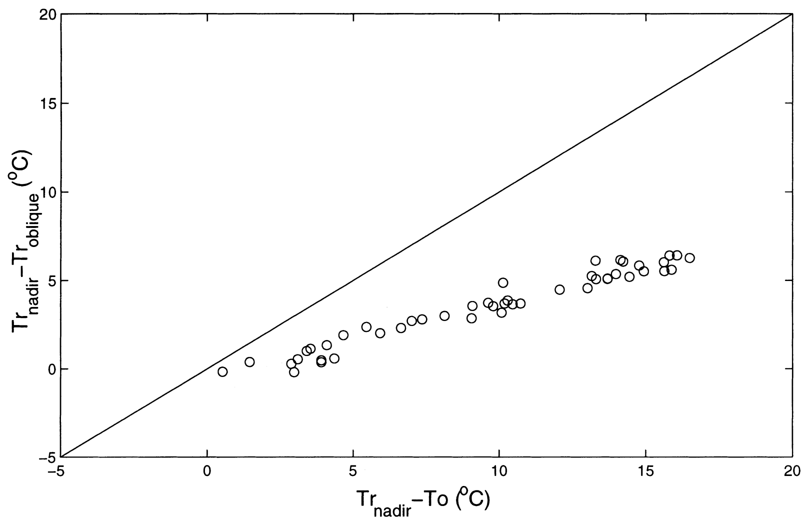

Fig. 5. Cross-plot of the difference between nadir viewing radiative and aerodynamic surface temperatures and the difference between nadir and off nadir radiative temperatures.

condition and vegetation status, which also impact soil and vegetation temperatures. In the same vein, differences between aerodynamic temperature and radiative temperature at nadir were plotted against the differences between nadir and oblique (55°C) viewing radiative temperature (Fig. 5). A strong linear relationship between the two differences exists. The slope and the correlation coefficient associated with the regression line, forced to the origin, was 2.60 and 0.92, respectively. This relationship is superior to that obtained in Chehbouni et al. (1996) where they reported a relationship between aerodynamic-radiative and radiative-air temperature differences which depends non-linearly on the PAI. Here, the slope of the line is constant despite the recorded variations in soil moisture and PAI values (see above). The status of surface soil moisture and vegetation condition, which control the departure of aerodynamic temperature from radiative temperature, is contained in nadir–oblique temperature differences (Chehbouni et al., 2001).

Based on the above observation, sensible heat flux can be reformulated as

$$H = \rho C_p \frac{[(T_\mathrm{r}(\theta_1) - T_\mathrm{a}) - \delta T]}{r_\mathrm{aa}} \quad \text{with } \delta T = T_\mathrm{r}(\theta_1) - T_0 \qquad (15)$$

where θ_1 is the nadir viewing angle. According to the observation made in Fig. 5, δT can be expressed in terms of the difference between nadir and oblique temperatures ΔT as

$$\delta T = \alpha \Delta T \qquad (16)$$

To validate this approach, a subset (10%) of the data was randomly selected to estimate the value of α through a regression line. The remaining data (90%) were used for the validation by comparing observed sensible heat flux values to those obtained using Eq. (15). The MAPD value was about 33%, which were not statistically very different from that obtained using the original two-layer model.

In an attempt to explain the constant value of the slope α, we found out that, due to the non-linearity associated with the radiance–temperature relationship, it was not possible to derive analytically an expression of the slope (α) using component surface temperatures inverted from Eqs. (14a) and (14b). Consequently, we assumed instead (for this particular purpose only) that directional radiative temperature can be approximated as a gap fraction weighted mean of soil and vegetation temperatures (Lhomme et al., 1994). Combining Eqs. (5)–(7), (15) and (16), and using the above assumption led to the following expression for the slope (α), where r_e and cc are two intermediate parameters defined as

$$\alpha = \frac{\mathrm{Tr}(\theta_1) - T_\mathrm{a}}{\Delta T} \frac{r_\mathrm{e}}{r_\mathrm{aa} + r_\mathrm{e}} + \mathrm{cc} \frac{r_\mathrm{aa}}{r_\mathrm{aa} + r_\mathrm{e}} \qquad (17)$$

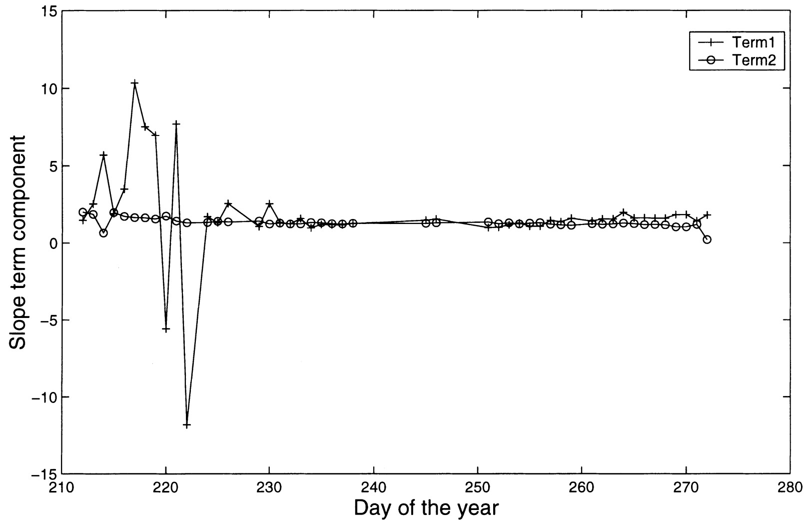

Fig. 6. Variation of the component terms of the slope α throughout the study period.

According to Eq. (17), α is composed of two terms. The first term from the left (called hereafter Term 1) depends on the ratio of the temperature differences as well as on that of the resistances, while the second term (called Term 2) depends solely on the ratio of resistances. These two terms when plotted separately against the DOY indicate they were of the same magnitude (Fig. 6). More importantly, besides a few outliers associated with Term 1, which where due to either negative or a very low temperature differences, both terms were constant throughout the study period. For further analysis, we examined the seasonal behavior of the individual components of each term. The result showed that Term 1 is dominated by the ratio of the temperatures which is mostly constant throughout the season. It also showed that none of the components of Term 2 is constant. Obviously there is a compensation effect to keep this term constant. This explained the experimental result depicted in Fig. 5. The “constant” value of the slope depends certainly on observational angles and canopy structure (leaf angle distribution, clumping factor, etc.). Detailed analysis of how changes of the above parameters influence the value of the slope needs to be performed. Nevertheless, this finding is of interest since it suggests that the dual angle thermal observations may provide a better alternative than a single angle one for characterizing aerodynamic temperature behavior.

5. Concluding remarks

The issue of estimating surface convective fluxes from remotely sensed radiative surface temperature has been heavily investigated during the past two decades. Still, no convincing approach for taking into account the difference between aerodynamic and radiative surface temperature has been developed over sparsely vegetated surfaces. All the reported approaches are empirical and therefore difficult to apply a priori to different surface types (Chehbouni et al., 2000a). The problem is that the departure of the aerodynamic temperature from the radiative temperature is controlled by several factors that are difficult to capture using a single viewing angle observation of surface temperature.

In this study, an approach based on the combination of dual angle observations of radiative temperature and a two-layer model has been used to estimate convective surface sensible heat fluxes over sparse grassland site in the San Pedro Basin. Comparison between observed and simulated flux leads to a MAPD of 23%, which can be considered reasonable knowing the difficulty associated with measuring convective fluxes over sparsely vegetated surfaces. However, the sensitivity analysis revealed that this approach required accurate values of measured directional radiative temperatures and the aerodynamic characteristics of the vegetation in order to perform properly.

Additional light has been shed on the relationship between aerodynamic and nadir viewing radiative surface temperature. The analysis showed that the difference between these two temperatures is well correlated with the difference between soil and vegetation temperatures. It also showed that this same difference is strongly correlated with the difference between nadir and oblique radiative temperatures. An analytical expression of the ratio between these two differences has been derived. It indicates that this ratio is constant despite the large variation of the recorded soil moisture and PAI values. This result is of interest since it suggests that dual angle observations of radiative surface temperature might be more effective for operational estimates of surface fluxes under varying conditions. However, additional analysis is needed to fully assess the potential and the limitation of this approach. In the future, this issue will be addressed through the use of a hydro-ecological model coupled to radiative transfer model, that allows for investigating the performance of this approach for different vegetation types and climatic conditions (Cayrol et al., 2000; Nouvellon et al., 2000b). Finally, the applicability of this approach over heterogeneous surfaces needs to be documented before it can be used with satellite data such as that provided by ATSR sensors.

Acknowledgements

We are grateful for funding from the European Union (WARTERMED Project: Contract # ICA3-CT-1999-00015) and CONACYT (Project: 29340T). Additional funding was provided by Landsat7 Science Team (NASA-S-1396-F), SALSA-global change program (NASA Grant W-18,997), and the French PNTS. Many thanks to F. Santiago, J.-C. Rodriguez and M. Jauri for their valuable help during the field experiment. We are grateful to Drs. Phil Heilman and Scot Miller for their helpful comments on the manuscript.

References

Arain, A.M., Michaud, J.D., Shuttleworth, W.J., Dolman, A.J., 1996. Testing of vegetation parameter aggregation rules applicable to the Biosphere–Atmosphere Transfer Scheme (BATS) at the Fife site. J. Hydrol. 177, 1–22.

Avissar, R., 1998. Which type of SVAT is needed for GCMs. J. Hydrol. 50, 3751–3774.

Bastiaansen, W.G.M., Menenti, M., Feddes, R.A., Holtslag, A.A.M., 1998. A remote sensing surface energy balance algorithm for land (Sebal). J. Hydrol. 212–213, 198–212.

Blumel, K., 1999. A simple formula for estimation of the roughness length for heat transfer over partly vegetated surfaces. J. Appl. Meteorol. 38, 814–829.

Brutsaert, W., 1982. Evaporation into the Atmosphere. Reidel, Dordrecht, Netherlands, 299 pp.

Brutsaert, W., Sugita, M., 1996. Sensible heat transfer parameterization for surfaces with anisothermal dense vegetation. J. Atmos. Sci. 53, 209–216.

Cahill, A.T., Parlange, M.B., 1997. On the Brutsaert temperature roughness length model for sensible heat flux estimation. Water Resour. Res. 10, 2315–2324.

Cayrol, P., Chehbouni, A., Kergoat, L., Dedieu, G., Mordelet, P., Nouvellon, Y., 2000. Grassland modeling and monitoring with SPOT-4 VEGETATION instrument during the 1997–1999 SALSA experiment. Agric. For. Meteorol. 105, 91–115.

Chehbouni, A., Lo Seen, D., Njoku, E.G., Monteny, B., 1996. Examination of the difference between radiative and aerodynamic surface temperatures over sparsely vegetated surfaces. Remote Sens. Environ. 58, 177–186.

Chehbouni, A., LoSeen, D., Njoku, E.G., Lhomme, J.-P., Monteny, B.M., Kerr, Y.H., 1997. Estimating of sensible heat flux using radiative surface temperature. J. Hydrol. 188, 855–868.

Chehbouni, A., Watts, C., Kerr, Y.H., Dedieu, G., Rodriguez, J.-C., Santiago, F., Cayrol, P., Boulet, G., Goodrich, D., 2000a. Methods to aggregate turbulent fluxes over heterogeneous surfaces: application to SALSA data set in Mexico. Agric. For. Meteorol. 105, 133–144.

Chehbouni, A., Goodrich, D.C., Moran, M.S., Watts, C.J., Kerr, Y.H., Dedieu, G., Kepner, W.G., Shuttleworth, W.J., Sorooshian, S., 2000b. A preliminary synthesis of major scientific results during the SALSA program. Agric. For. Meterol. 105, 311–323.

Chehbouni, A., Nouvellon, Y., Kerr, Y.H., Moran, M.S., Watts, C., Prevot, L., Goodrich, D.C., Rambal, S., 2001. Directional effect on radiative surface temperature measurements over semi-arid grassland. Remote Sens. Environ., in press.

Choudhury, B.J., Monteith, J.L., 1988. A four-layer model for the heat budget of homogeneous land surfaces. Quart. J. Roy. Meteorol. Soc. 114, 373–398.

Crago, R.D., 1998. Radiometric and equivalent isothermal surface temperatures. Water Resour. Res. 34, 3017–3023.

Francois, C., Ottle, C., Prevot, L., 1997. Analytical parameterization of canopy directional in the thermal infrared. Application on the retrieval of soil and foliage temperatures using two-diretional measurements. Int. J. Remote Sens. 12 (18), 2587–2621.

Goodrich, D.C., Chehbouni, A., Goff, B., et al., 2000. Preface to the semi-arid land-surface-atmosphere (SALSA) Program (Special issue). Agric. For. Meteorol. 105, 3–20

Hall, G.H., Huemmrich, K.F., Goetz, S.J., Sellers, P.J., Nickeson, J.E., 1992. Satellite remote sensing of surface energy balance: success, failure and unresolved issues in FIFE. J. Geophys. Res. 97, 19061–19089.

Humes, K.S., Kustas, W.P., Moran, M.S., Nichols, W.D., Weltz, M.A., 1994. Variability of emissivity and surface temperature over sparsely vegetated surface. Water Resour. Res. 30, 1299–1310.

Kalma, J.D., Jupp, D.L.B., 1990. Estimating evaporation from pasture using infrared thermometry: evaluation of a one-layer resistance model. Agric. For. Meteorol. 51, 223–246.

Kimes, D.S., 1980. Effect of vegetation canopy structure on remotely sensed canopy temperatures. Remote Sens. Environ. 10, 165–174.

Kimes, D.S., 1981. Remote sensing of temperature profiles in vegetation canopies using multiple view angle and inversion techniques. IEEE Trans. Geosci. Remote Sens. GE-19 (2), 85–90.

Kubota, A., Sugita, M., 1994. Radiometrically determined skin temperature and scalar roughness to estimate surface heat flux. Part I. Parameterization of radiometric scalar roughness. Bound.-Lay. Meteorol. 69, 397–416.

Kustas, W.P., Norman, J.M., 1997. A two-source approach for estimating turbulent fluxes using multiple angle thermal infrared observations. Water Resour. Res. 33, 1495–1508.

Kustas, W.P., Choudhury, B.J., Moran, M.S., Reginato, R.J., Jackson, R.D., Gay, L.W., Weaver, H.L., 1989. Determination of sensible heat flux over sparse canopy using thermal infrared data. Agric. For. Meteorol. 44, 197–216.

Kustas, W.P., Choudhury, B.J., Inoue, Y., Pinter, P.J., Moran, M.S., Jackson, R.D., Reginato, R.J., 1990. Ground and aircraft infrared observations over a partially vegetated area. Int. J. Remote Sens. 3, 409–428.

Lhomme, J.P., Monteny, B., Chehbouni, A., Troufleau, D., 1994. Determination of sensible heat flux over Sahelian fallow savannah using infra-red thermometry. Agric. For. Meteorol. 68, 93–105.

Lhomme, J.P., Troufleau, D., Monteny, B., Chehbouni, A., Bauduin, S., 1997. Sensible heat flux–radiometric surface temperature over sparse Sahelian vegetation. II. A model for the kB^{-1} parameter. J. Hydrol. 188–189, 839–854.

Lhomme, J.P., Chehbouni, A., Monteny, B.M., 2000. Sensible heat flux–radiometric surface temperature relationship over sparse vegetatin: parameterizing the B^{-1} parameter. Bound.-Lay. Meteorol. 97 (3), 431–457.

Malhi, Y., 1996. The behaviour of the roughness length for temperature over heterogeneous surfaces. Quart. J. Roy. Meteorol. Soc. 122, 1095–1125.

Massman, W.J., 1999. A model study of kB_H^{-1} for vegetated surfaces using “localized near-field” Lagrangian theory. J. Hydrol. 223, 27–43.

Mathias, A.D., Yates, S.R., Zhang, R., Warrick, A.W., 1987. Radiant temperatures of sparse plant canopies and soil using IR thermometry. IEEE Trans. Geosci. Remote Sens. 25, 516–519.

Moran, M.S., Kustas, W.P., Vidal, A., Stannard, D.I., Blanford, J.H., Nichols, W.D., 1994. Use of ground-based remotely sensed data for surface energy balance evaluation of a semi-arid rangeland. Water Resour. Res. 30, 1339–1349.

Njoku, E.G., Hook, S.J., Chehbouni, A., 1996. Effects of surface heterogeneity on thermal remote sensing of land parameters, Chapter 2. In: Stewart, J.B., Engman, E.T., Feddes, R.A., Kerr, Y. (Eds.), Scaling up in Hydrology Using Remote Sensing. West Sussex, UK, John Wiley & Sons, pp. 19–31.

Norman, J.M., Kustas, W.P., Humes, K.S., 1995. Source approach for estimating soil and vegetation energy fluxes in observations of directional radiometric surface temperature. Agric. For. Meteorol. 77, 263–293.

Nouvellon, Y.P., Bégué, A., Moran, M.S., Lo Seen, D., Rambal, S., Luquet, D., Chehbouni, A., Inoue, Y., 2000a. PAR extinction in shortgrass-ecosystems: effects of clumping, sky conditions and soil albedo. Agric. For. Meteorol. 105, 21–41.

Nouvellon, Y., Moran, M.S., Chehbouni, A., Lo Seen, D., Bryant, R., Nichols, M., Prévot, L., Rambal, S., Ni, W., Bégué, A., Heilman, P., Keefer, T.O., 2000b. Assimilating LANDSAT data in an ecosystem model for multi-year simulation of grassland carbon, water and energy budget. In: Proceedings of the IGARSS, Honolulu, Hawaii, July 24–28, 2000, 4 pp.

Paulson, C.A., 1970. The mathematical representation of wind speed and temperature profiles in the unstable atmospheric surface layer. J. Appl. Meteorol. 9, 857–861.

Prata, A.J., 1990. Land surface temperature derived from AVHRR and ATSR. I. Theory. J. Geophys. Res. 98, 16689–16702.

Prevot, L., 1985. Modelisation des echanges radiatifs au sein des couverts vegetales: application a la teledetection. Validation sur un couvert de mais. Ph.D. Dissertation. University of Paris, Paris.

Shaw, R.H., Pereira, A.R., 1982. Aerodynamic roughness of a plant canopy: a numerical experiment. Agric. For. Meteorol. 26, 51–65.

Shuttleworth, W.J., Gurney, R.J., 1990. The theoretical relationship between foliage temperature and canopy resistance in sparse crop. Quart. J. Roy. Meteorol. Soc. 116, 497–519.

Shuttleworth, W.J., Wallace, J.S., 1985. Evaporation from sparse crops — an energy combination theory. Quart. J. Roy. Meteorol. Soc. 111, 839–855.

Stewart, J.B., Kustas, W.P., Humes, K.S., Nichols, W.D., Moran, M.S., De Bruin, H.A.R., 1994. Sensible heat flux–radiometric surface temperature relationship for eight semi-arid areas. J. Appl. Meteorol. 33, 1110–1117.

Sugita, M., Brutsaert, W., 1996. Optimal measurement strategy for surface temperature to determine sensible heat flux from anisothermal vegetation. Water Resour. Res. 32, 2129–2134.

Sugita, M., Kubota, A., 1994. Radiometrically determined skin temperature and scalar roughness to estimate surface heat flux. Part II. Performance of parameterized scalar roughness for the determination of sensible heat. Bound.-Lay. Meteorol. 70, 1–12.

Sun, J., Mahrt, L., 1995. Determination of surface fluxes from the surface radiative temperature. J. Atmos. Sci. 52, 1096–1106.

Troufleau, D., Lhomme, J.-P., Monteny, B., Vidal, A., 1997. Sensible heat flux and radiometric surface temperature over sparse sahelian vegetation: is the kB^{-1} a relevant parameter. J. Hydrol. 189, 815–838.

Verhoef, A., de Bruin, H.A.R., van den Hurk, B.J.J.M., 1997. Some practical notes on the parameter kB^{-1} for sparse vegetation. J. Appl. Meteorol. 36, 560–572.

Watts, C.J., Chehbouni, A., Rodriguez, J.-C., Kerr, Y.H., Hartogensis, O., De Bruin, H.A.R., 2000. Comparison of sensible heat flux estimates using AVHRR with scintillometer measurements over semi-arid grassland in northwest Mexico. Agric. For. Meteorol. 105, 81–89.